

Inhibition, kinetic and thermodynamic effects of new Azo derivatives on iron corrosion in acidic and alkaline solutions

*¹Loutfy H. Madkour and ²Zinhome UA

¹Chemistry Department, Faculty of Science and Arts, Baljarashi, Al-Baha University, P.O.Box. (1988), Al-Baha, Kingdom of Saudi Arabia

²Chemistry Department, Faculty of Science, Tanta University, 31527, Tanta, Egypt

*Corresponding author E-mail: loutfy_madkour@yahoo.com; Tel. +966 541945518; Fax: +966 77247272

Accepted 14 December 2014

Abstract

This investigation is designed to apply an advanced kinetic-thermodynamic model on the experimental data obtained from acidic and alkaline corrosion of iron using mono- and bis-azo dyes as corrosion inhibitors. The inhibition properties of the tested azo dyes on corrosion of iron in HNO₃ and NaOH media were analyzed by gravimetric, thermometric and polarization measurements. The three studied methods gave consistent results. Polarization study showed that all the inhibitors are mixed type in acidic, act mainly as cathodic in alkaline solution. The synthesized azo dye derivatives exhibit good inhibition properties, obeys the Frumkin adsorption isotherm. The large values of the change in the standard free energy of adsorption (ΔG_{ads}°), equilibrium constant (K_{ads}) and binding constant (K_b) revealed that the reactions proceed spontaneously and result in highly efficient physisorption mechanism and stronger electrical interaction between the double layer existing at the phase boundary and the adsorbing molecules. The inhibition efficiency depends on the number of adsorption oxygen sites (OH and OMe groups), their charge density and π -electron clouds. The inhibition efficiency evaluated via theoretical methods was well accorded with reported experimental ones, following the same order as: α -naphthyl- ligand > β -naphthyl > *p*-anisidine > *p*-toluidine > *o*-toluidine > *m*-toluidine derivative. This research might provide a theoretical inhibition performance evaluation approach for homologous inhibitors.

Keywords: Corrosion, inhibitor, mono- and bis-azo dyes, iron, HNO₃, NaOH

INTRODUCTION

Among numerous anticorrosion measures, corrosion inhibitor is widely used and acts as one of the most economical and effective ways [1-3]. A number of organic compounds [4-7] are known to be applicable as corrosion inhibitors for iron and its alloys in acidic environments. Such compounds contain nitrogen, oxygen or sulphur in a conjugated system can donate one pair of electrons, and multiple bonds, and function via adsorption of the molecules on the metal surface, creating barrier against corrosion attack [8-14]. The adsorption bond strength depends on the composition of the metal and corroding inhibitor structure and concentration as well as temperature. The corrosion inhibition of iron in 2.0 M HNO₃ and 2.0 M NaOH solutions has been reported recently by using Schiff bases [15]. Generally, localized corrosion can be prevented by the action of adsorptive inhibitors which prevent the adsorption of the aggressive anions or by the formation of oxide films on the metal surface [15-22]. It has been observed that the adsorption of these inhibitors depends on the physico-chemical properties of the functional groups and the electron density at the donor atom. The

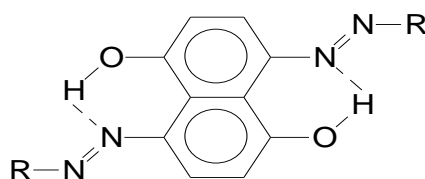
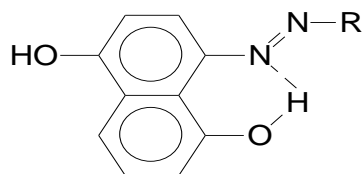
adsorption occurs due to the interaction of the lone pair and/or π -orbitals of inhibitor with d-orbitals of the metal surface atoms, in which the metal acts as an electrophile and the inhibitor acts as a Lewis base whose nucleophilic centers are O and/or N atoms with free electronic pairs which are readily available for sharing, which evokes a greater adsorption of the inhibitor molecules onto the surface, leading to the formation of a corrosion protection film [15, 20-25]. Furthermore, adsorption and consequently the efficiency of an inhibitor donot only depend on its structure, but also on the characteristics of the environment in which it acts, the nature structure, the charge of metal surface and other experimental conditions [26]. The choice of effective inhibitors is based on their mechanism of action and electron-donating ability. The significant criteria involved in this selection are molecular structure, electron density on the donor atoms, solubility and dispersibility [27-30]. In any case, adsorption is general over the metal surface and the resulting adsorption layer function as a barrier, isolating the metal from the corrosion [31]. The inhibition efficiency has found to be closely related to inhibitor adsorption abilities and molecular properties for different kinds of organic compounds [32]. Previously, some work has been done in our laboratory on these bis-and mono-azo dyes whereas; the compounds are successful as corrosion inhibitors on aluminum and zinc metals in hydrochloric acid and sodium hydroxide [33]. The choice of these (MAD) and (BAD) as inhibitors is based on the following considerations: these molecules (a) can be easily synthesized from relatively cheap materials, (b) $-N=N-$ group, electronegative oxygen and aromatic rings as active centers (c) and have high solubility in acidic and alkaline media. The action of such investigated (MAD) and (BAD) inhibitors depend on the specific interaction between the functional groups and the metal surface. The present study was undertaken to investigate the inhibition of iron corrosion in 2.0 M HNO_3 and NaOH by these two newly synthesized series (MAD) and (BAD) derivatives. The study was conducted by using weight loss, thermometric, electrochemical polarization measurements and confirmed by using kinetic and thermodynamic calculations.

MATERIALS AND METHODS

Synthesis of mono-and bis-azo dye (MAD) and (BAD) inhibitors

The investigated azo dye derivatives were synthesized by diazotization of primary aromatic amines and coupling with the corresponding naphthol derivatives in the ratio 1:1 and 2:1 in the case of (MAD) and (BAD) respectively. The compounds are purified and characterized by 1H NMR, IR spectroscopy and element analysis before use [33]. The inhibitor solutions were prepared by dissolving the appropriate amount in 10 cm³ Analar ethanol. The desired volume of the free inhibitor was added to the electrolyte solution. The ratio of ethanol was kept constant for each test. This stock solution was used for all experimental purposes.

The molecular structure of (MAD) and (BAD) is given below:



R
 α -Naphthyl(1)
 β -Naphthyl (2)
 C_6H_4OMe-p (3)
 C_6H_4Me-p (4)
 C_6H_4Me-o (5)
 C_6H_4Me-m (6)

R
 α -Naphthyl(7)
 β -Naphthyl(8)
 C_6H_4OMe-p (9)
 C_6H_4Me-p (10)
 C_6H_4Me-o (11)

It is evident that (MAD) and (BAD) are aromatic compounds containing nitrogen and oxygen atoms, which could easily be protonated in acidic solution, and several π -electrons exist in these molecules.

Electrodes and electrolytes

The corrosion tests were performed on a freshly prepared iron specimens of the following composition (in wt.%): 0.091% C, 0.002% Si, 0.196% Mn, 0.011% P, 0.016% S, 0.009% Cr, 0.021% Ni, 0.01% Al, 0.024% Cu and Fe balance. The test

specimens used in the weight loss measurements were mechanically cut into (2.0 cm x 2.0 cm x 0.1 cm) dimensions, for thermometric study, specimens were cut into (10.0 cm x 1.0 cm x 0.1 cm) sizes and for electrochemical study, specimens was soldered with Cu-wire for electrical connection and mounted into the epoxy resin to offer only one active flat surface exposed to the corrosive environment. Before each experiment, the electrode was first mechanically abraded with a sequence of emery papers of different grades (320, 400, 800, 1000, and 1200), respectively, followed by washing with double distilled water and finally degreased in absolute ethanol and acetone, dried in room temperature and stored in a moisture free desiccators before their use in corrosion studies [15,20,22,33-36]. The corrosive solutions, 2.0 M HNO₃ and 2.0 M NaOH were prepared by dilution of analytical grade reagents with double distilled water. The concentration range of employed inhibitors was (5 x 10⁻⁴ to 0.1 mM) in 2.0 M HNO₃ and 2.0 M NaOH.

Measurements

Three methods weight loss assessment, thermometric, and electrochemical polarization curves were used to determine the corrosion inhibition efficiencies of (MAD) and (BAD) for iron corrosion in acidic and alkaline solution.

Weight loss measurements

Weight loss experiments were done according to the standard methods as reported in literature. The corrosion rates, C_R (mg cm⁻² h⁻¹) were calculated according to the following equation [37]:

$$CR = W/Dta \quad (1)$$

Where W is the average weight loss of three parallel iron sheets (one specimen in each beaker), a is the total surface area of the iron specimen, t is the immersion time and D is the density of iron specimen. The inhibition efficiency ($In\%$) was calculated using the following equation [38]:

$$In\% = [(C_{R(uninh)} - C_{R(inh)}) / C_{R(uninh)}] \times 100 \quad (2)$$

where $C_{R(uninh)}$ and $C_{R(inh)}$ are the values of corrosion rates (mg cm⁻² h⁻¹) obtained of iron in uninhibited inhibited solutions, respectively.

Weight loss measurements were conducted under total immersion using 250 mL capacity beakers containing 200 mL test solution at 303 K maintained in a thermo stated water bath. The iron specimens were weighed accurately (using Mettler AG104 0.1 mg Analytical Balance) and suspended in the beaker with the help of rod and hook. The specimens were immersed in 250 mL beaker contained 200 mL 2.0 M HNO₃ and/or 2.0 M NaOH with and without addition of different concentrations (5 x 10⁻⁷ – 1 x 10⁻⁴ M) of the tested inhibitors. After different immersion time intervals of (0.5, 1.0, 1.5, 2.0, 2.5, 3.0, 3.5, 4.0, 4.5, 5.0, 5.5 and 6.0 h), the iron specimens were taken out, washed, dried, and weighed accurately. The average weight loss tests at a certain time were repeated for each of the three pieces of iron specimens. The specimens were immersed in the solutions without blocking any side, and the whole specimen area was considered in the calculation.

Thermometric measurements

The reaction vessel used was basically the same as that described by Mylius [39]. An iron piece specimens were cut into (10.0 cm x 1.0 cm x 0.1 cm) sizes were immersed in 30 cm³ of 2M HNO₃ and/or 2M NaOH in the absence and presence of inhibitors respectively. The temperature of the system was followed as a function of time. The reaction number (RN) and the reduction in reaction number (% red RN) were calculated using the following Eqs. (3) and (4):

$$RN = (T_{max} - T_i) / t \quad (3)$$

$$\% \text{ red } RN = [(RN_{(uninh)} - RN_{(inh)}) / RN_{(uninh)}] \times 100 \quad (4)$$

where T_{max} and T_i , are the maximum and initial temperatures, respectively, t is the immersion time (in minutes) required to reach T_{max} , $RN_{(uninh)}$ and $RN_{(inh)}$ are the reaction number in the absence and presence of inhibitors, respectively [15,20,33,40]. The specimens were immersed in the solutions without blocking any side.

Polarization measurements

Potentiostatic polarization experiments were carried out using a standard electrochemical three-electrode cell [15, 20, 22, 33, 34]. Iron acts as working electrode (WE), saturated calomel electrode (SCE) as reference electrode and platinum was used as counter electrode, which was separated from the main cell compartment by a glass sinter and an iron rod working electrode with a fine lugging capillary placed close to the working electrode to minimize ohm resistance. In order to avoid contamination, the reference electrode was connected to the working-electrode through a salt bridge filled with the test solution. The tip of the bridge was pressed against the working electrode in order to compensate the ohmic

drop. In deaerated electrochemical tests, the solution under investigation was 25 cm³ deoxygenated with nitrogen of high purity before tests for 4 h while the flow of the gas in the solution was continued during the measurements. The bubbling rate, which was not measured, was small and the same which could be ignored in all the experiments. Measurements were performed on a planar disk electrode (A= 1cm²). The edges of the working electrode were masked by appropriate resins (Duracryle, Spofa-Dental, and Praha). The electrodes were rinsed in an ultrasonic bath containing double distilled water before being immersed in the cell. The polarization measurements were carried out using a laboratory potentiostat (Wenking Potentioscan model POS 73, Germany). In this method, the working electrode was immersed in test solution for 45 min until the open circuit potential was reached. After that the working electrode was polarized in both cathodic and anodic directions. The obtained values of (current-potential) were fitted, and the polarization curves were then plotted. The values of corrosion current density (i_{Corr}) were calculated from the extrapolation of straight part of the Tafel lines. The potential increased with respect to the open circuit potential vs.corrosion potential (E_{Corr}). The inhibition efficiency ($In \%$) was defined as:

$$In\% = [(i_{Corr(uninh)} - i_{Corr(inh)}) / i_{Corr(uninh)}] \times 100 \quad (5)$$

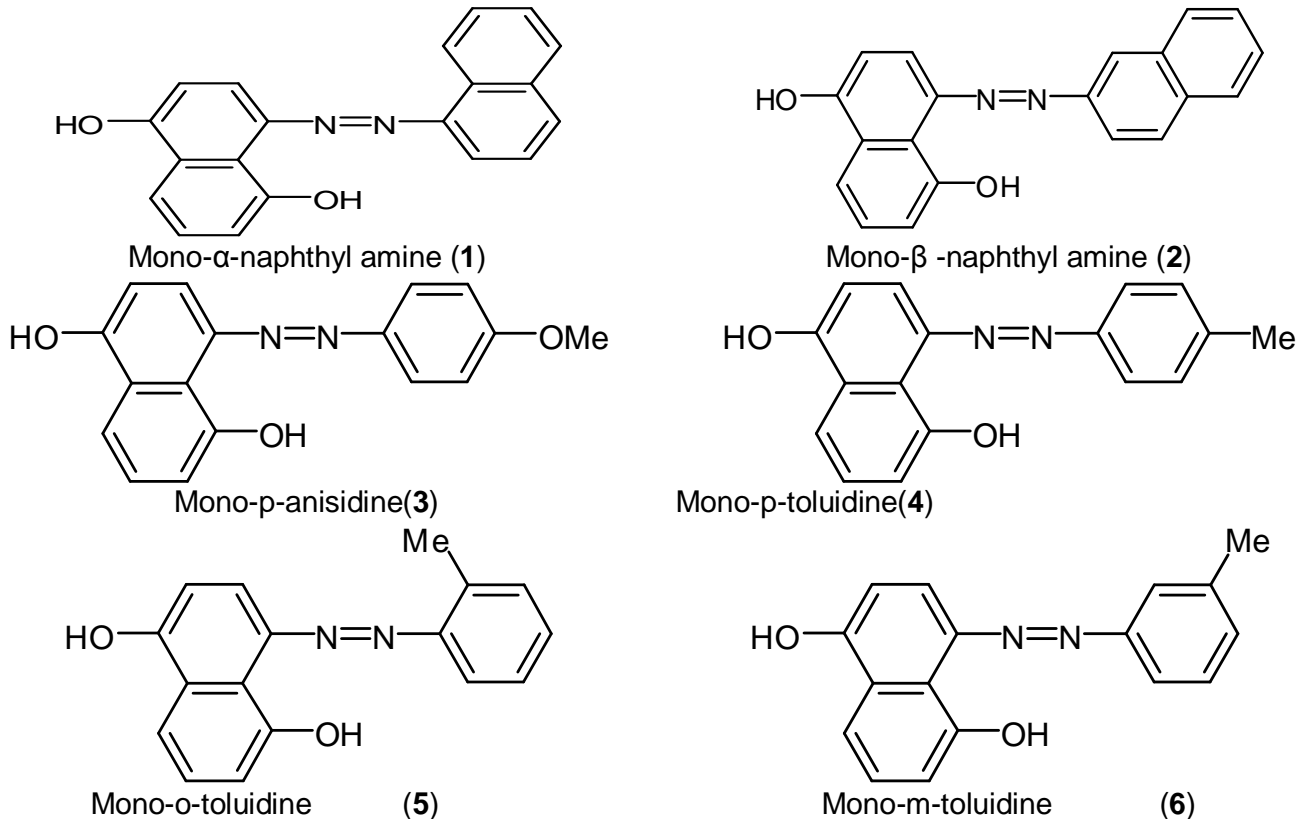
Where $i_{Corr(uninh)}$ and $i_{Corr(inh)}$ are the corrosion current density values without and with inhibitors. The cell temperature was kept constant at 303.0 ± 1.0 K in an ultra-thermostat.

RESULTS AND DISCUSSION

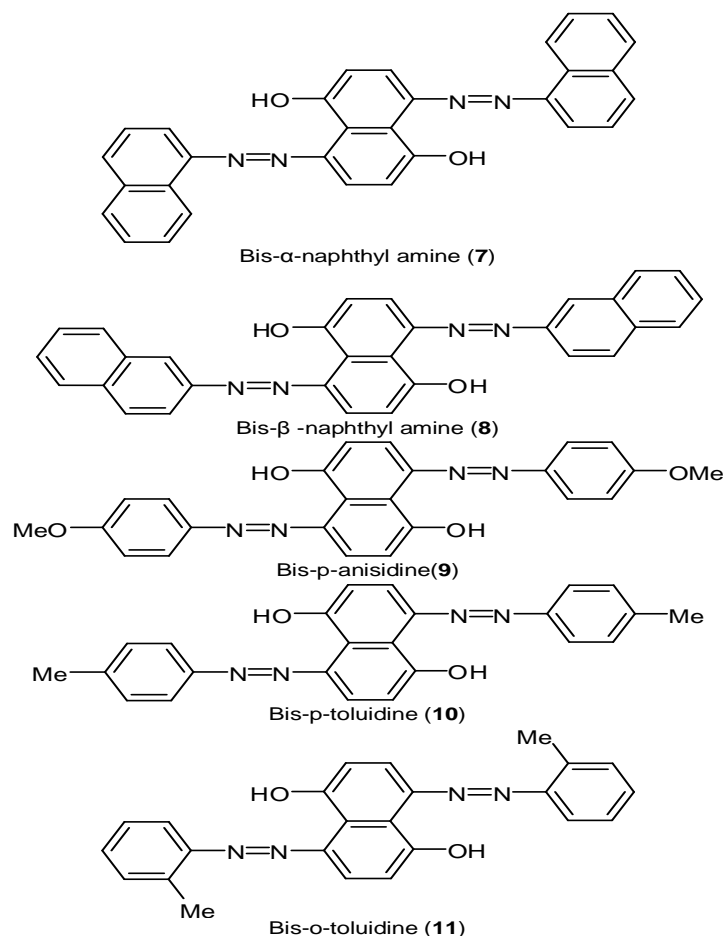
Corrosion inhibition performance of the synthesized inhibitors can be evaluated using electrochemical and chemical techniques.

Structure of mono- and bis- azo dyes

The chemical structures of the synthesized inhibitors (MAD) and (BAD) were confirmed using ¹H NMR, IR spectroscopy and elemental analysis. The molecular structures of the studied (MAD) and (BAD) derivatives are illustrated in the following Schemes 1 and 2, respectively:



Scheme 1. Molecular structures of the studied synthesized mono-azo dye derivatives



Scheme 2. Molecular structures of the studied synthesized bis-azo dye derivatives

Weight loss measurements

Gravimetric evaluation of the synthesized inhibitors and the effect of inhibitor dose, for the chemical methods, a weight loss measurement are ideally suited for long term immersion test. Corroborative results between weight loss and other techniques have been reported [41-43]. At present, weight loss is probably the most widely used method of inhibition assessment [15, 35-36, 44-48]. It is the most accurate and precise method for determining metal corrosion rate because the experimentation is easy to replicate and, although long exposure times may be involved, the relatively simple procedure reduces the propensity to introduce systematic errors. The anodic dissolution of iron in acidic media and the corresponding cathodic reaction has been reported to proceed as follows [49]:



As a result of these reactions, including the high solubility of the corrosion products, the metal loses weight in the solution. The effect of addition of different (MAD) and (BAD) derivatives at various concentrations on the iron corrosion in 2.0 M HNO_3 and 2.0 M NaOH solution was studied by weight loss measurements at 303 K. Table 1 represents the corrosion inhibition efficiencies (In%) of the synthesized inhibitors (at 5×10^{-7} – 1×10^{-4} M) on the iron corrosion in 2.0 M HNO_3 solution at 303 K. The extent of covering the metal surface by inhibitor molecules can be expressed in terms of the surface coverage (θ) which represents the degree of arrangement of inhibitor molecules on the metal surface [50]:

$$\theta = 1 - (W_i / W_0) \quad (8)$$

where W_i and W_0 are the weight losses of the iron specimens in presence and absence of inhibitors respectively. It is clear that the gradual increase of the inhibitor dose from 5×10^{-7} to 1×10^{-4} M increases the adsorbed molecules onto

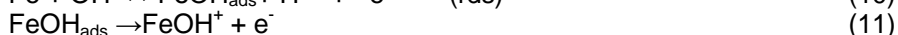
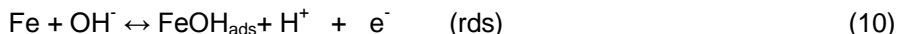
the metal surface, which increases the surface coverage and the inhibition efficiencies of tested inhibitors (Table 1). This effect may be attributed to the accumulation of the inhibitor molecules onto the metal surface, which decreases the interaction between the acidic medium and the metal surface. The adsorption of inhibitor molecules onto the metal surface occurred due to the interaction between the negatively charged centre of the metal surface and the positively charged head groups (N^+), and π -electrons of the inhibitor molecules. It is reported that the hetero atoms facilitate the adsorption of inhibitor molecules at the metal surface due to the electronegativity factor [51, 52]. The inhibition tendency of the corrosion inhibitors is increased in presence of the hetero atoms in the following sequence: $S > N > O$ [53]. The high inhibition tendency of the tested inhibitors may be attributed to the presence of the nitrogen and oxygen atoms in their chemical structure. The nitrogen atoms participated in the azo group is protonated in the acidic medium, which enhances their adsorption onto the metal surface. The maximum inhibition efficiencies were obtained at 1×10^{-4} M for (MAD) and (BAD) derivatives at 303 K. From Table 1, it is clear that the order of inhibition efficiency obtained from weight loss measurements of (MAD) and (BAD) is as follows:

α -naphthyl- ligand > β -naphthyl > p -anis dine > p -toluidine > o -toluidine > m -toluidine derivative.

It is apparent from the gravimetric data in Table 1 that the gradual increase of the inhibitor dose decreases the corrosion rates. The lowest corrosion rate of iron was obtained at 1×10^{-4} M of the synthesized inhibitors. The adsorbed inhibitor molecules at higher doses form a well arranged monolayer on iron metal surface where the organic parts (alkyl chains) are arranged to locate the medium and the head groups attached to the metal surface, that inhibits the metal-acid reaction to large extent [54]. Figure 1 shows corrosion loss of weight-loss measurement as a function of time. Weight-loss in mg cm^{-2} of the iron surface area was determined in an open system under unstirred conditions in 2.0 M HNO_3 and 2.0 M NaOH solution at time intervals. The observed curves in Figure 1 (a) are characterized by a rapid rise at the first hour from immersion, and then the curves are followed by slow rise. The observed corrosion parameters values depend on the nature and concentration of the applied corrosive medium. The observed curves in nitric acid solution (Figure 1 (a)) confirm the pre-immersion oxide film formed on the iron surface gives no protection against nitric acid attack. The weight loss-time curves observed in alkaline medium show a gradual continuously small definite increasing of weight loss as the time of immersion increases, give straight lines starting from the origin (Figure 1 (b)), this is because of the oxide film which originally formed at the electrode surface was easily detectable in NaOH medium. Thus, the dissolution of iron itself in 2.0 M NaOH solution is linearly to the reaction time (at 303 K). This behaviour is an indication of zero order reaction with general equation (Eq. (9)).

$$W_t = kt \quad (9)$$

Where Wt is the weight loss of iron at time t and k is the rate constant. The values of k can be calculated from the slope of the $W_t - t$ curves at the given temperature. In this manner k of iron dissolution in NaOH and in the presence of the inhibitors were determined. The values of k can also be used for comparing the inhibition efficiencies of the inhibitors. It is obvious that the loss in weight in the presence of the investigated (MAD) and (BAD) is lower than that in its absence, and mostly decreases as the concentration of the additives increased from $5 \times 10^{-7} - 1 \times 10^{-4}$ M; consequently, (θ) and $(\% \text{In})$ increases as denoted by the decrease in weight loss values. The weight loss-time curves for the tested synthesized azo dye derivatives (Figure 1) fall below that of the free corrosive media. Thus, both (MAD) and (BAD) act as strong inhibitors. The corrosion rate of iron in nitric acid medium is under anodic control [55] which is:



where 'red' stands for rate-determining step.

The adsorption isotherm experiments were performed to have more insights into the mechanism of corrosion inhibition, since it describes the molecular interaction of the inhibitor molecules with the active sites on the iron surface [56]. The surface coverage, θ , was calculated according to the previous equation (8). The surface coverage values (θ) for different inhibitor concentration were tested by fitting to various isotherms and the models considered were [57]:

$$\text{Temkin isotherm } \exp(f \cdot \theta) = k_{\text{ads}} \cdot C \quad (13)$$

$$\text{Langmuir isotherm } (\theta/1 - \theta) = k_{\text{ads}} \cdot C \quad (14)$$

$$\text{Frumkin isotherm } (\theta/1 - \theta) \exp(-2f \cdot \theta) = k_{\text{ads}} \cdot C \quad (15)$$

$$\text{Freundlich isotherm } \theta = k_{\text{ads}} \cdot C \quad (16)$$

Where k_{ads} is the equilibrium constant for adsorption process, C is the concentration of inhibitor and f is the energetic inhomogeneity. Attempts were made to fit the θ values to various isotherms including Langmuir, Temkin, Frumkin and Freundlich. By far the best fit is obtained with the Frumkin adsorption isotherm [58]. The plot of (θ) vs. $\log C$ gave S-

shaped curves as shown in Figure 2. Stabilizing effect [59] that comes from the complex compound formed indicates rearrangement of the charge density inside the molecule, thus shows its corrosion inhibition. This is supported by U.V. spectrophotometer analysis and also conductivity measurements.

Table 1

A) Corrosion parameters obtained from weight loss measurements for iron in 2.0 M HNO³ containing various concentrations of the synthesized mono-azo dye (MAD) inhibitors at 303 K

(6)		(5)		(4)		(3)		(2)		(1)		Inhibitor
(% In)	θ	(% In)	θ	(% In)	θ	(% In)	θ	(% In)	θ	(% In)	θ	C mol
61.0	0.610	61.0	0.610	61.3	0.613	64.3	0.643	64.7	0.647	64.7	0.647	5 × 10 ⁻⁷
61.6	0.616	61.1	0.611	61.5	0.615	64.4	0.644	65.6	0.656	67.1	0.671	1 × 10 ⁻⁶
62.6	0.626	61.3	0.613	62.4	0.624	64.6	0.646	65.9	0.659	67.6	0.676	5 × 10 ⁻⁶
64.4	0.644	64.5	0.645	65.4	0.654	65.7	0.657	67.2	0.672	68.5	0.685	1 × 10 ⁻⁵
71.1	0.711	71.1	0.711	72.0	0.720	72.9	0.729	73.3	0.733	74.6	0.746	5 × 10 ⁻⁵
73.5	0.735	74.0	0.740	75.0	0.750	76.4	0.764	77.6	0.776	78.5	0.785	1 × 10 ⁻⁴

B) Corrosion parameters obtained from weight loss measurements for iron in 2.0 M HNO³ containing various concentrations of the synthesized bis-azo dye (BAD) inhibitors at 303 K

(11)		(10)		(9)		(8)		(7)		Inhibitor
(% In)	θ	(% In)	θ	(% In)	θ	(% In)	θ	(% In)	θ	C mol dm ⁻³
60.1	0.601	62.1	0.621	63.1	0.631	63.4	0.634	64.4	0.644	5 × 10 ⁻⁷
60.4	0.604	62.2	0.622	63.5	0.635	63.6	0.636	64.5	0.645	1 × 10 ⁻⁶
60.7	0.607	64.8	0.648	64.9	0.649	63.9	0.639	64.6	0.646	5 × 10 ⁻⁶
62.7	0.627	65.8	0.658	65.7	0.657	65.5	0.655	66.2	0.662	1 × 10 ⁻⁵
70.0	0.700	70.9	0.709	71.2	0.712	71.3	0.713	73.3	0.733	5 × 10 ⁻⁵
74.8	0.748	76.2	0.762	76.7	0.767	78.9	0.789	80.0	0.800	1 × 10 ⁻⁴

Table 2. Effect of different concentrations of (MAD) inhibitor (1) on the thermometric parameters of Fe in 2M HNO₃

C mol dm ⁻³	θ/C°	θ _{max} /C°	t/min	Δt/min	Log (Δt/min)	θ	RN/C° min ⁻¹	% red. in RN
0	19.5	50.8	68	----	----	----	0.460	---
5 × 10 ⁻⁷	18.5	46.5	122	54	1.732	0.502	0.229	50.2
1 × 10 ⁻⁶	18	46.0	130	62	1.792	0.532	0.215	53.2
5 × 10 ⁻⁶	18	40.9	143	75	1.875	0.652	0.160	65.2
1 × 10 ⁻⁵	18	39.9	145	77	1.886	0.671	0.151	67.2
5 × 10 ⁻⁵	18	39.0	180	112	2.049	0.746	0.116	74.7
1 × 10 ⁻⁴	18	37.4	196	128	2.107	0.786	0.098	78.7

Table 3. Comparison between the inhibition efficiency of (MAD and (BAD) derivatives in 2M HNO₃ and 2M NaOH solutions as determined by weight loss, thermometric and polarization methods at (1 × 10⁻⁴ M inhibitor concentration) and 303 K

Inhibitor	Corrosion Inhibition Efficiency (% In)					
	Weight loss		Thermometric		Polarization	
	HNO ₃	NaOH	HNO ₃	NaOH	HNO ₃	NaOH
I₁ (MAD)	79	45	78.7	----	77.8	58.5
I₂	78	51	77.7	----	76.4	61.4
I₃	76	43	74.8	----	75.9	50.5
I₄	75	40	74.2	----	72.1	45.1
I₅	74	38	74.0	----	69.4	42.1
I₆	73	34	69.6	----	69.3	38.1
II₇ (BAD)	80	58	77.1	----	78.4	65.1
II₈	79	55	76.2	----	76.6	63.1
II₉	77	54	77.3	----	76.0	61.3
II₁₀	76	53	74.3	----	74.6	54.1
II₁₁	75	49	73.7	----	73.1	50.1

Table 4. Fitting parameters of the kinetic-thermodynamic model and the Frumkin adsorption isotherms of the synthesized (MAD) and (BAD) inhibitors in 2.0 M HNO₃ and 2.0 M NaOH solutions at 303K

Inhibitor	Medium	Kinetic model			Frumkin isotherm		
		1/y	K _b	-ΔG ^o _{ads} kJ mol ⁻¹	-f	K _{ads}	-ΔG ^o _{ads} kJ mol ⁻¹
I ₁ (MAD)	HNO ₃	8.57	2.16x10 ⁸	38.21	23.42	36307	16.33
	NaOH	2.86	4707.10	11.18	40.46	8394	12.64
I ₂	HNO ₃	8.98	2.01x10 ⁸	38.03	23.70	34593	16.20
	NaOH	2.71	11636.71	13.46	36.70	9772	13.03
I ₃	HNO ₃	9.50	1.92x10 ⁸	37.91	24.08	32359	16.04
	NaOH	1.99	4042.06	10.80	41.44	7568	12.38
I ₄	HNO ₃	8.40	4.48x10 ⁷	34.25	24.52	29991	15.81
	NaOH	3.45	1614.81	8.49	44.03	6745	12.09
I ₅	HNO ₃	8.86	4.43x10 ⁷	34.22	24.85	28444	15.71
	NaOH	5.39	1164.87	7.67	45.86	6151	11.86
I ₆	HNO ₃	9.57	7.52x10 ⁷	35.55	25.03	27669	15.64
	NaOH	4.44	980.97	7.23	50.73	5058	11.37
II ₇ (BAD)	HNO ₃	52.63	6.5x10 ¹⁸	98.94	23.00	39994	16.56
	NaOH	2.19	29104.15	15.77	31.50	13803	13.89
II ₈	HNO ₃	30.31	1.4x10 ¹²	60.25	23.27	37153	16.41
	NaOH	3.76	26309.37	15.51	33.31	12022	13.55
II ₉	HNO ₃	20.79	2.3x10 ¹¹	55.77	23.97	32359	16.04
	NaOH	4.29	19319	14.74	33.96	11748	13.49
II ₁₀	HNO ₃	28.90	1.4x10 ¹¹	54.49	22.75	11220	15.98
	NaOH	4.56	10917.50	13.30	33.35	12722	13.69
II ₁₁	HNO ₃	23.25	4.3x10 ¹⁰	51.55	24.58	29512	15.81
	NaOH	2.61	8561.79	12.69	38.10	9462	12.94

*Correlation coefficient (0.94)

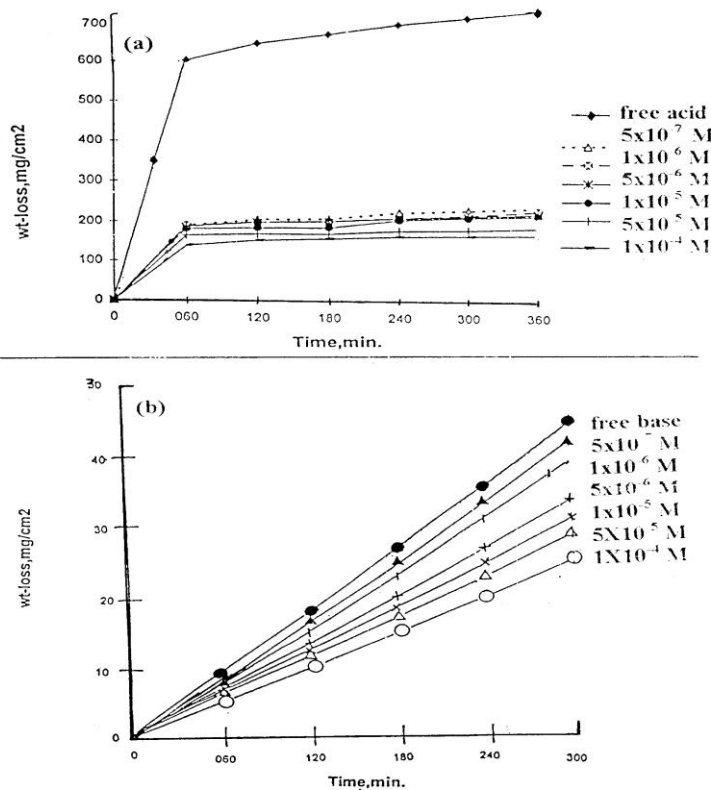


Fig.1. Weight loss vs. time curves of iron corrosion in the absence and in the presence of different concentrations of inhibitor I(1) in (a) 2M HNO₃ acid and (b) 2M NaOH at 303 K.

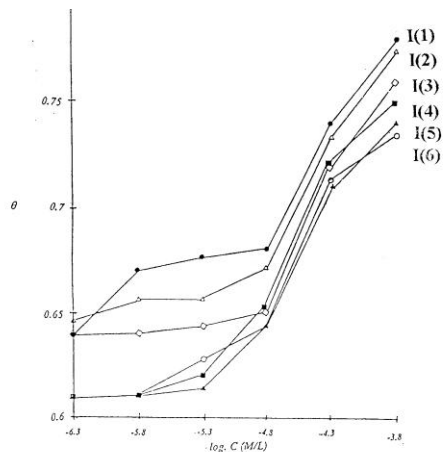


Fig.2. Variation of iron surface coverage (θ) with the logarithmic concentration of different substituted azo additives in 2M HNO_3 acid at 303 K .

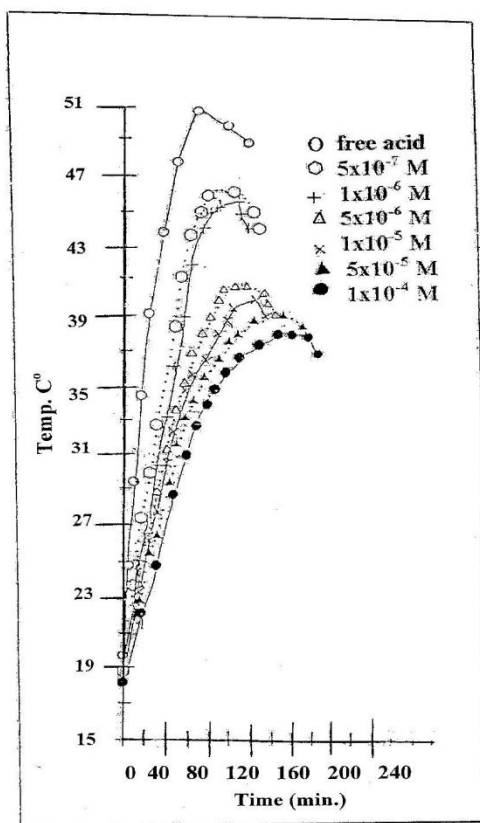


Fig.3. Temperature vs. time curves of iron corrosion in 2M HNO_3 in presence of different concentrations of (MAD) inhibitor (1).

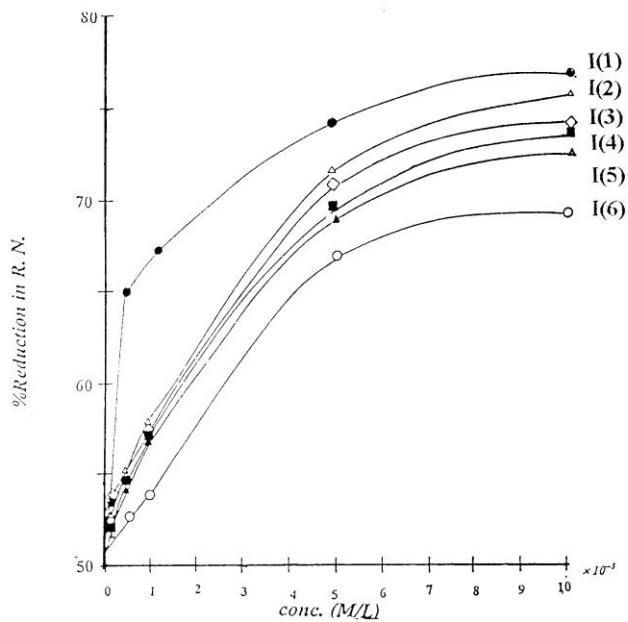


Fig.4. Effect of substituted azo derivatives concentration on percentage reduction in reaction number (% red. in RN) of iron corrosion in 2M HNO₃ acid .

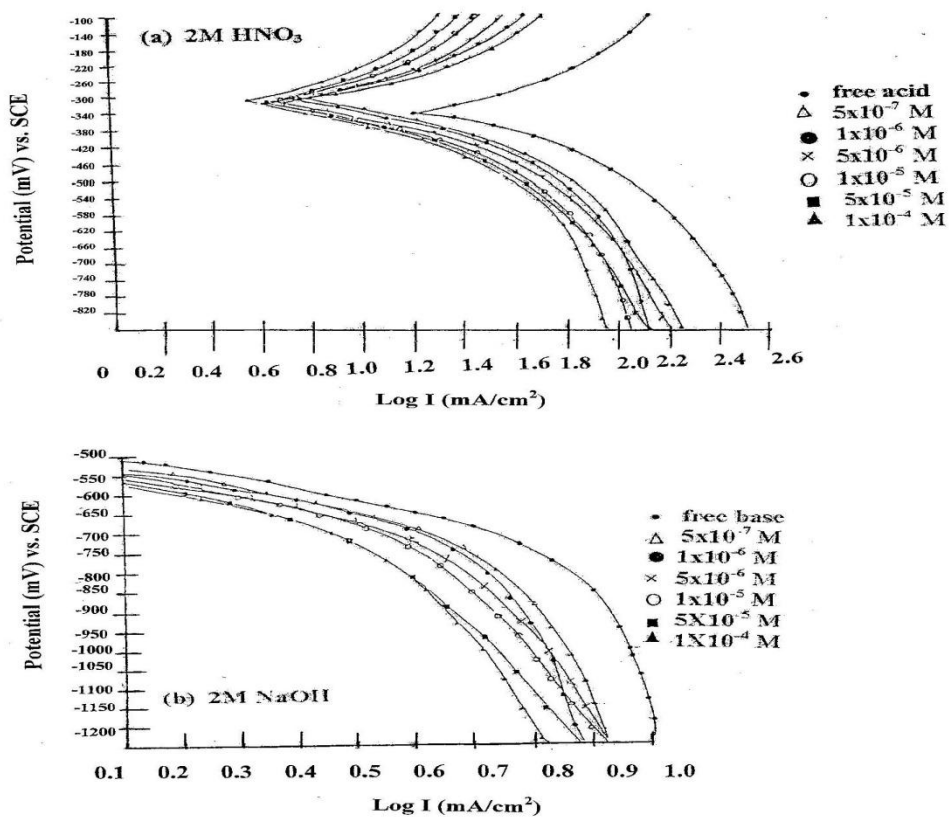


Fig.5. Polarization curve of iron corrosion in presence of different concentrations of (MAD) inhibitor (I) in (a) 2 M HNO₃ and (b) 2M NaOH at 30 C°.

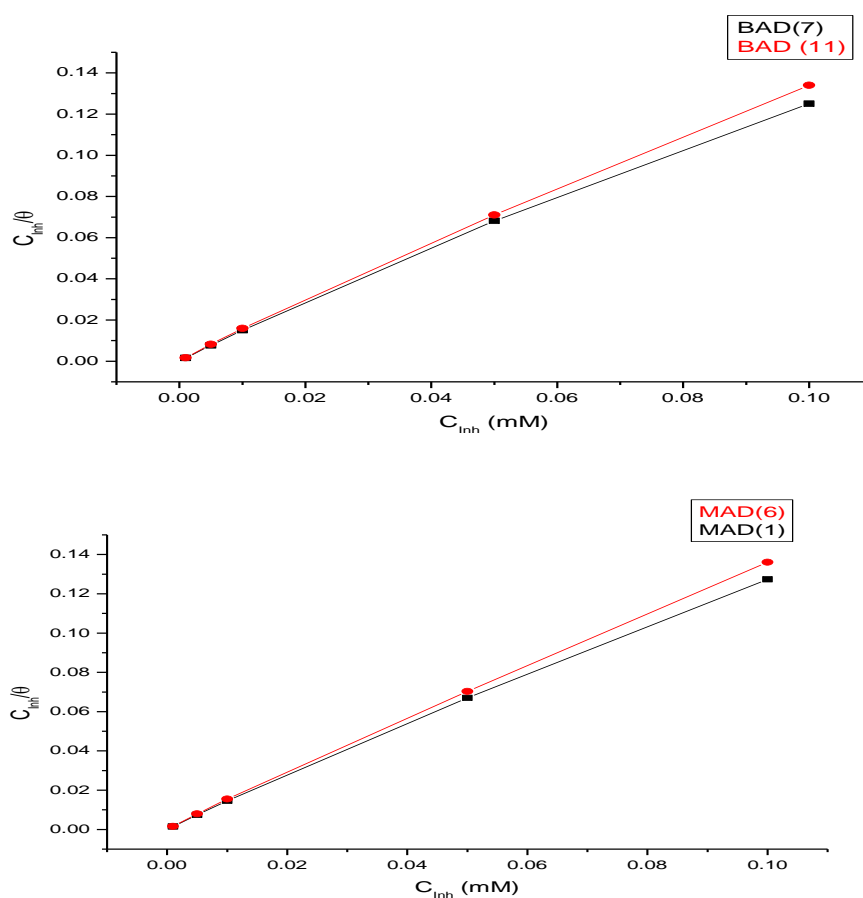


Figure 6. Relation between C_{inh} and C_{inh}/θ of the synthesized bis-azo dye (7), (11) and mono-azo dye (1), (6) for iron in 2.0 M HNO_3 at 30°C

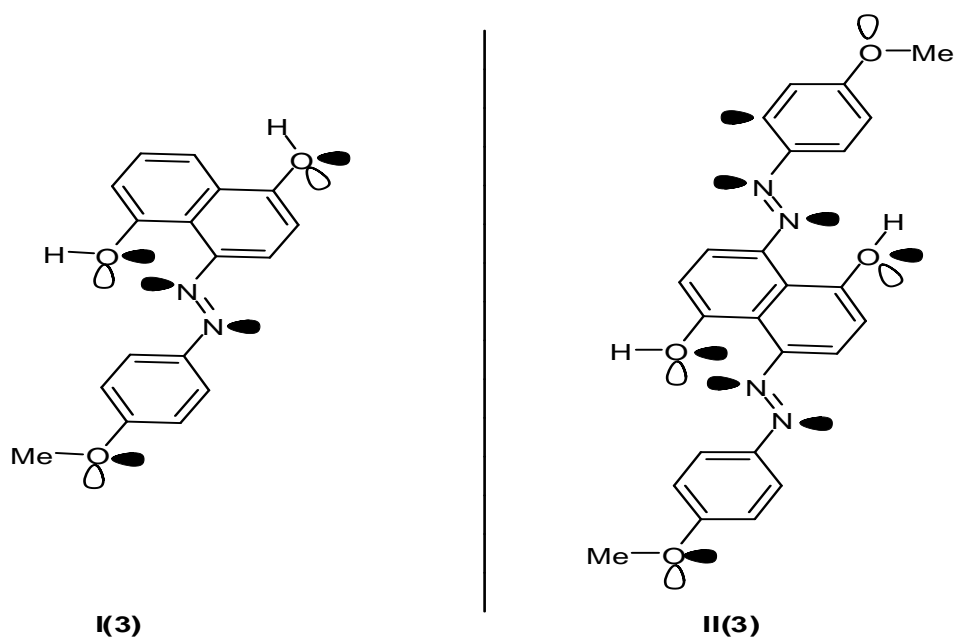


Figure 7. Skeletal representation of the proposed mode of adsorption of mono-*p*-anisidine (3) and bis-*p*-anisidine (9)

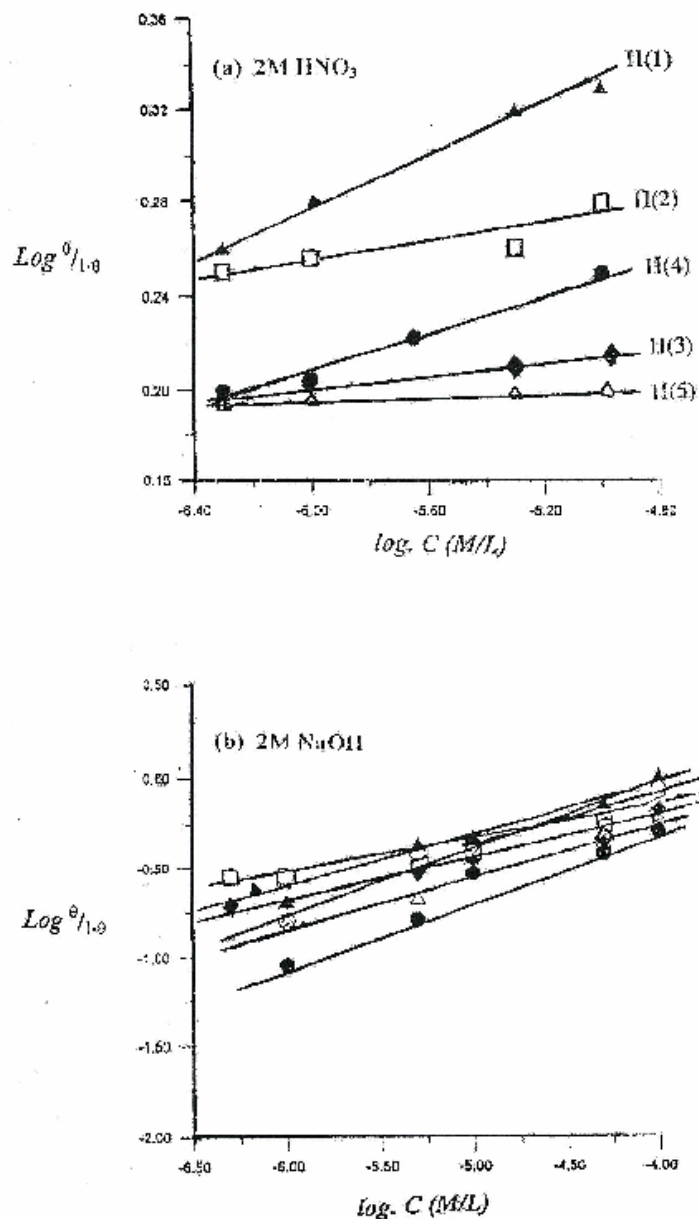


Fig.8. Application of kinetic-thermodynamic model on mono- and bis-azo inhibitors of iron in (a) 2M HNO₃ acid and (b) 2M NaOH at 303 K.

Thermometric measurements

In this method the temperature change of the system involving iron dissolution in 2.0 M HNO₃ was followed without and with different concentrations of the investigated (MAD) and (BAD) derivatives, as given in Figure 3 for compound (1) as an example for all additives. An incubation period is first recognized along which the temperature rises gradually with time. The temperature-time curves provide a mean of differentiating between weak and strong adsorption. The thermometric data are depicted in Table 2. It is evident that, the dissolution of iron in 2.0 M HNO₃ starts from the moment of immersion. On increasing the concentration of the inhibitor from ($5 \times 10^{-7} - 1 \times 10^{-4}$ M) the value of T_{\max} decreases, whereas the time (t) required reaching T_{\max} increases, and both factors cause a large decrease in (RM) and increasing of (% red RM) of the system [39], as shown in Table 2. This indicates that the studied synthesized azo dye additives retard the dissolution presumably by strongly adsorption onto the metal surface. The extent of inhibition depends on the degree of the surface coverage (θ) of the iron surface with the adsorbate. Iron, as an active element, always carries an

air formed oxide, which specifically and very strongly adsorbs H^+ and OH^- ions according to the equations (10-12), these reactions takes place along the incubation period. The heat evolved from the above reactions accelerates further dissolution of the oxide and activates the dissolution of the iron metal exposed to the aggressive medium.

The relation between RN , time delay (Δt) and/or $\log(\Delta t)$ versus molar concentration of the additives confirms a two-step adsorption process [60], at first a monolayer of the adsorbed is formed on the iron electrode surface, and then it is followed by the adsorption of a second adsorbed layer or a chemical reaction leading to the deposition of the (azo dye-Fe complex) on the metal surface. The plot of Δt and/or $\log(\Delta t)$ as a function of $\log C_{in}$ yields a linear relation shape for the first region of the curve then a region of constancy; this reveals the completion of the adsorbed monolayer of the inhibitor. In thermometric measurements (% red RN_{in}) values are taken as the measure for the corrosion inhibition efficiency (% In). Plots of % red RN versus molar concentration (C_{in}) of the additives for iron corrosion in 2.0 M HNO_3 are invariably sigmoidal in nature as shown in Figure 4. The inhibition efficiency of the synthesized (MAD) and (BAD) derivatives depends on many factors, including the molecular size, heat of hydrogenation, mode of interaction with iron electrode surface, formation of metallic complexes and the charge density on the adsorption sites. Adsorption is expected to take place primarily through functional groups, essentially OH and OCH_3 would depend on its charge density as reported [61]. The thermometric technique is not applied for the dissolution of iron in sodium hydroxide because of the temperature changes of the system involving iron immersed in 2.0 M NaOH solution was varied but with a negligible change. This is due to the fact that the oxide film originally formed on the iron electrode surface is easily detectable in 2.0 M NaOH.

Tafel polarization curves measurements

Electrochemical measurement is considered to be a fast and efficient method which reflects the transient electrochemical process, so it can be used for measuring corrosion rate on-site, because from the shape of the experimental curve it may be possible to obtain important information on the kinetics of the corrosion reactions. Fig.5 shows Tafel polarization curves of iron in 2.0 M HNO_3 and 2.0 M NaOH in the absence and presence of different concentrations of (MAD) inhibitor (1) at 303 K (as an example). As seen from Fig.5 (a) and (b), the anodic and cathodic Tafel slopes are changed in small range and independent on the inhibitors concentrations, indicating that the inhibition role of these inhibitors is not through the interference on the reactions of metal dissolution and reduction of protons. This indicates that the (MAD) and (BAD) derivatives act as adsorptive inhibitors, i.e., they reduce anodic dissolution and also retard the hydrogen evolution reaction [62] via blocking the active reaction sites on the iron surface, or even can screen the covered part of the electrode; and therefore protect it from the action of the corrosion medium [63].

This effect is attributed to the adsorption of the inhibitor on the active sites of the iron surface. The values of corrosion current, corrosion potential, cathodic and anodic Tafel slopes are obtained by the anodic and cathodic regions of the Tafel plots. The corrosion current density (i_{corr}) can be obtained by extrapolating the Tafel lines to the corrosion potential and the inhibition efficiency (%In) values were calculated from Eq.(5). It is obvious that the slopes of the cathodic (β_c) Tafel lines almost changed in small values upon addition of the tested azo dye derivatives. The parallel cathodic Tafel lines suggested that the addition of inhibitors to the 2.0 M HNO_3 solution do not modify the hydrogen evolution mechanism and the reduction of H^+ ions at the iron surface which occurs mainly through a charge-transfer mechanism. The shift in the anodic Tafel slope (β_a) values may be due to the adsorption of nitrate ions/or inhibitor modules onto the iron surface [64]. It is also clear that there is a shift towards cathodic region in the values of corrosion potential (E_{corr}), from the fact that $\beta_c > \beta_a$. The extent of adsorption of inhibitor molecules onto the metal surface in term of the surface coverage (θ) was calculated using Eq. (17) [65]:

$$\theta = (i_{Corr(uninh)} - i_{Corr(inh)}) / i_{Corr(uninh)} \quad (17)$$

where $i_{Corr(uninh)}$ and $i_{Corr(inh)}$ are the corrosion current densities in the absence and presence of the inhibitors, respectively. It is clear from the polarization curves that the increase of the inhibitor concentrations decreases the corrosion current (i_{Corr}) which consequently increases the surface coverage values. Also, the corrosion current density (i_{Corr}) of iron corrosion reaction is decreased by increasing the inhibitor dose. In this respect, the decrease in current density in presence of the different synthesized inhibitors reveals that the corrosion reaction proceeded much slower than the uninhibited medium. Moreover, the gradual increase in the inhibitor doses considerably decreases the corrosion current densities. Comparing the corrosion currents and the inhibition efficiencies of the used inhibitors shows that increasing the inhibitor doses decreases the corrosion currents, and consequently increases the retardation of the iron dissolution in the acidic and alkaline media. The results show that (MAD) (1) and (BAD) (7) inhibitors at 1×10^{-4} M produce the lowest corrosion current densities (7.713, 7.488 $mA\ cm^{-2}$) and the maximum inhibition efficiencies obtained were 77.8% and 78.4% respectively (Table 3). In literature, it has been reported that if the displacement in E_{corr} (i) is > 85

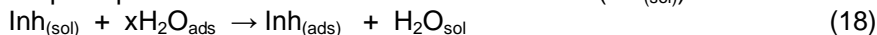
mV with respect to E_{corr} , the inhibitor can be seen as a cathodic or anodic type and (ii) if displacement in E_{corr} is < 85 mV, the inhibitor can be seen as mixed type. In our study the maximum displacement in E_{corr} value was 45 mV towards cathodic region, which indicates that all studied (MAD) and (BAD) derivatives are mixed-type (anodic/cathodic) inhibitors [66-68] in 2.0 M HNO_3 , cause anodic and cathodic over potential and inhibit both the hydrogen evolution and anodic dissolution processes. The inhibitors act mainly as cathodic type in 2.0 M NaOH as seen in Figure 5 (b), whereas the maximum displacement in E_{corr} value was 129 mV towards cathodic region. The cathodic reduction of the passive film on iron in 2.0 M NaOH results in the formation of a non reducible porous layer. The surface layer was found to grow also during cathodic polarization; actually the cathodically polarized surface can be covered with $\text{Fe}(\text{OH})_2$, as given previously in equations (10-12). Results indicate that, the cathodic reaction is the rate-determining step and all the investigated additives predominantly under cathodic control and act mainly as cathodic inhibitors from the blocking adsorption type. The magnitude of the displacement of Tafel plots is proportional to the inhibitor concentration. The inhibition efficiency strongly depends on the structure and chemical properties of the layers formed at the electrode surface under prevailing experimental conditions. Increase in inhibition efficiencies with the increase of concentrations of studied (MAD) and (BAD) derivatives shows that the inhibition actions are due to its adsorption on iron surface [69,70]. The increase in the inhibition efficiencies of iron, in 2.0 M HNO_3 solution, with increasing additive concentration can be explained on the basis of additive adsorption. The higher inhibition efficiencies values for additives in 2.0 M HNO_3 with respect to NaOH is due to the less negative potential of iron in acid solution, favoring adsorption of the additive on the metal electrode surface. The sequence of % In obtained from the polarization measurements are as follows:

α -naphthyl- ligand $> \beta$ -naphthyl $> p$ -anis dine $> p$ -toluidine $> o$ -toluidine $> m$ -toluidine derivative.

The inhibition efficiencies calculated from potentiostatic polarization curves are in good agreement with those obtained from weight loss and thermometric measurements as shown in Table 3. This agreement confirms the validity of the present chemical and electrochemical measurements also support the explanation given for the effect of chemical composition on the inhibitive action of the tested synthesized (MAD) and (BAD) derivatives. Nevertheless, they showed small differences in their absolute (% In) values, could be attributed to the different experimental conditions under which each technique was carryout.

Adsorption isotherm and thermodynamic consideration

Generally speaking, corrosion inhibitors are found to protect iron corrosion in acid and alkaline solutions by adsorbing themselves on iron surface. Moreover, the adsorption process depends on the molecule's chemical composition, the temperature and the electrochemical potentials at the metal/solution interface. The adsorption isotherms describe the behaviour of the inhibitor molecules and provide information about the interaction of the inhibitor molecules with the electrode surface [71-73]. The adsorption of inhibitors at the metal-solution interface is represented as a substitution adsorption process between the inhibitor molecules ($\text{Inh}_{(\text{sol})}$) and the water molecules on metallic surface ($\text{H}_2\text{O}_{\text{ads}}$):



Where $\text{Inh}_{(\text{sol})}$ and $\text{Inh}_{(\text{ads})}$ are the inhibitor species dissolved in the aqueous solution and adsorbed onto the metallic surface, respectively. $\text{H}_2\text{O}_{(\text{ads})}$ is the water molecules adsorbed on the metal surface and x is the ratio which represents the number of water molecules replaced by a single inhibitor molecule. Fitting of the gravimetric measurement data describes the mode of interaction occurred between the inhibitor molecules and the metal surface. Adsorption is a separation process involving two phases between which certain components can be described by two main types of interaction [74]: (1) physisorption which involves electrostatic forces between ionic charges at the metal/solution interface. The heat of adsorption is low and therefore this type of adsorption is stable only at relatively low temperatures and; (2) chemisorptions which involves charge sharing or charge transfer from the inhibitor molecules to the metal surface to form a coordinate type bond. In fact electron transfer is typically for transition metals having vacant low-energy electron orbital. Chemisorptions is typified by much stronger adsorption energy than physical adsorption. Such a bond is therefore more stable at higher temperatures.

Basic information on the adsorption of inhibitor on metal surfaces can be provided by adsorption isotherm. Attempts were made to fit experimental data to various isotherms including Frumkin, Langmuir, Temkin, Freundlich, Bockris-Swinkels and Flory-Huggins isotherms. All these isotherms are of the general form [75]:

$$f(\theta, x) \exp(-2\alpha\theta) = K_{\text{ads}} C \quad (19)$$

where $f(\theta, x)$ is the configurational factor which depends on the physical mode and the assumptions underlying the derivation of the isotherm, θ the degree of surface coverage, C the inhibitor concentration, x the size factor ratio, α the molecular interaction parameter, and K_{ads} the equilibrium constant of the inhibitor adsorption process. In this study, correlation coefficient (R^2) was used to determine the best fit isotherm which was obtained from Frumkin adsorption isotherm. According to this isotherm, θ is related to the inhibitor concentration by the following equation [76]:

$$\exp(-2\alpha\theta) = K_{\text{ads}} C \quad (20)$$

where the molecular interaction parameter α can have both positive and negative values. Positive values of α indicates attraction forces between the adsorbed molecules while negative values indicate repulsive forces between the adsorbed molecules [76]. Upon rearrangement of Eq. (20), the following equation is obtained:

$$\theta = [1/(-2\alpha)] \ln(K_{ads}C) \quad (21)$$

If the parameter f is defined as:

$$f = -2\alpha \quad (22)$$

where f is the heterogeneous factor of the metal surface describing the molecular interactions in the adsorption layer and the heterogeneity of the metal surface. Eq. (22) clearly shows that the sign between f and α is reverse, that is, if $\alpha < 0$, then $f > 0$; if $\alpha > 0$, then $f < 0$. Accordingly, if $f > 0$, mutual repulsion of molecules occurs and if $f < 0$ attraction takes place. If Eq. (22) is substituted into Eq. (21), then the Frumkin isotherm equation [77] has the following form:

$$\theta = (1/f) \ln(K_{ads}C) \quad (23)$$

where θ is the degree of surface coverage, and could be calculated by the following relationship [78]:

$$\theta = \% \ln/100 \quad (24)$$

Eq. (23) can be transformed into:

$$\theta = (1/f) \ln K_{ads} + (1/f) \ln C \quad (25)$$

Eq. (25) is a different form of the Frumkin isotherm. The plot of θ versus $\ln C$ gives a S-shaped graph, suggest that the adsorption of the investigated synthesized (MAD) and (BAD) derivatives on the iron obeyed the Frumkin adsorption isotherm. Straight lines of C_{inh}/θ versus C_{inh} plots indicate that the adsorption of the inhibitor molecules on the metal surface obeyed Frumkin adsorption model (Fig.6). This isotherm can be represented as:

$$C_{inh}/\theta = 1/K_{ads} + C_{inh} \quad (26)$$

The strong correlation coefficients of the fitted curves are around unity ($r > 0.985$). This reveals that the inhibition tendency of the inhibitors is due to the adsorption of these synthesized molecules on the metal surface [79] (Table 4). The slopes of the C_{inh}/θ versus C_{inh} plots are close to ≈ 1.3 which indicates the ideal simulating and expected from Frumkin adsorption isotherm [79]. K_{ads} values were calculated from the intercepts of the straight lines on the C_{inh}/θ axis [80]. The relatively high values of the adsorption equilibrium constant (K_{ads}) as given in Table 4, reflect the high adsorption ability of these molecules on iron surface. The value of K_{ads} is related to the standard free energy of adsorption (ΔG_{ads}°) by the following Eq.(27).

$$K_{ads} = (1/55.5) \exp(-\Delta G_{ads}^{\circ}/RT) \quad (27)$$

where R is the universal molar gas constant ($\text{kJ mol}^{-1}\text{K}^{-1}$) and T is the absolute temperature (K). The value of 55.5 is the molar concentration of water in solution expressed in mol L^{-1} . The calculated values of ΔG_{ads}° and K_{ads} of the synthesized (MAD) and (BAD) inhibitors were listed in Table 4. The negative values of ΔG_{ads}° indicating the spontaneously adsorption of these molecules on the metal surface [81] and strong interactions between inhibitor molecules and the metal surface [82]. Generally, values of ΔG_{ads}° around -20 kJ mol^{-1} or lower are consistent with the electrostatic interaction between charged organic molecules and the charged metal surface (physisorption); while those around -40 kJ mol^{-1} or higher involve charge sharing or transfer from the organic molecules to the metal surface to form a co-ordinate type of bond (chemisorptions) [83-85]. The values of ΔG_{ads}° for both (MAD) and (BAD) compounds on iron in 2.0 M HNO_3 and 2.0 M NaOH solutions are tabulated in Table 4, being around -20 kJ mol^{-1} indicate a physical adsorption, i.e., physisorption mechanism. In addition to electrostatic interaction, there may be some other interactions [86, 87]. The high K_{ads} and ΔG_{ads}° values may be attributed to higher adsorption of the inhibitor molecules at the metal-solution interface [88]. In physisorption process, it is assumed that acid anions such as NO_3^- ions are specifically adsorbed on the metal surface, donating an excess negative charge to the metal surface. In this way, potential of zero charge becomes less negative which promotes the adsorption of inhibitors in cationic form [89].

Mode of adsorption

The mechanism of the inhibition processes of the corrosion inhibitors under consideration is mainly the adsorption one. The process of adsorption is governed by different parameters almost depend on the chemical structure of these inhibitors. The presence of nitrogen and oxygen in the organic structures makes the formation of $\pi\text{-}\pi$ bond resulting from overlap of 3d electrons from Fe atom to the 2p half or non-completely filled orbital of the nitrogen and oxygen atoms possible, which enhances the adsorption of the compounds on the metal surface. These molecules are able to adsorb on the metal surface through N and O atoms, azo groups and aromatic rings which are electron donating groups [90]. Adsorption of the studied (MAD) and (BAD) molecules on iron surface interferes with the adsorption of the anions NO_3^- and OH^- present in acid and alkaline solutions respectively. The inhibitor molecule, also can undergo the formation of a chelate complex (Fe-inhibitor complex) with Fe^{3+} ions resulting in the corrosive media, and will be readily adsorbed or deposited on the metal surface. The inhibition efficiencies increase with increasing the inhibitor concentration, molecular weight and immersion time, while it decreasing with increasing temperature. It was found that, the mode of

adsorption depends on the affinity of the iron metal towards the π – electron clouds of the ring system [60]. Fe has a greater affinity towards aromatic moieties; hence it adsorbs benzene rings in a flat orientation. The better performance of (BAD) derivatives is due to high electron density and large surface area which leads to more adsorption on the iron surface, also large sized molecules can provide better surface coverage and better inhibition efficiency.

Skeletal representation of the proposed mode of adsorption of the investigated (MAD) and (BAD) inhibitors is shown by Figure (7), which clearly indicates that the active adsorption centers. Among the compounds investigated in this study, mono-*p*-anisidine (3) and bis-*p*-anisidine (9) has been found to give the best performance. This can be explained on the basis that compound (3) can be chemisorbed as a tridentate surface ligand. However, the inhibitor (9) is adsorbed in a flat orientation through a tetra dentate form. The surface coordination is through the oxygen atoms from both the OH and OCH₃ groups which rises the possibility of transferring the unshared electron of these molecules to iron in comparison to other derivatives and therefore results in a better adsorption [91]. It was concluded that, the mode of adsorption depends on the affinity of the iron metal towards the π -electron clouds of the ring system [60]. Iron has greater affinity towards aromatic moieties were found to adsorb benzene rings in a flat orientation as shown in Figure (7). The order arrangement of increasing the corrosion inhibition efficiency of the (MAD) and (BAD)inhibitors on iron in 2.0 M HNO₃ and 2.0 M NaOH solutions was as follows:

α -naphthyl amine (1) > β -naphthyl amine (2) > *p*-anisidine (3) > *p*-toluidine (4) > *o*-toluidine (5) > *m*-toluidine (6) (MAD) substituents, and:

α -naphthyl amine (7) > β -naphthyl amine (8) > *p*-anisidine (9) > *p*-toluidine (10) > *o*-toluidine (11) (BAD) derivatives.

Compounds (1) and (7) are the most efficient inhibitors of the investigated (MAD) and (BAD), respectively. This seems to be adsorbed on the iron surface through each of adsorption oxygen centers and π -electron system of the benzene rings. It was found that, substituted phenyl rings in the α -position for both mono- and bis-azo derivatives (1) and (7) increases longitudinal polarization of the π -electron clouds. Thus, the adsorbed species lie flat on the iron surface causing a higher inhibitive effect value than the others derivatives. When the phenyl rings lies in the β -position for compounds (2), (8), this is because transverse polarization and consequently their adsorption are relatively decreased on the metal surface. The adsorption of inhibitors (3), (9) depends on the three oxygen adsorption sites. Methyl (CH₃-) group is more basic than the H-atom, so its presence within the azo dyes molecule causing increasing the localization of the π -electron clouds on the Fe metal surface depending on its position as follows: *p* > *o* > *m*-position. Thus, compound (4) lie before (5) and the compound (6) comes at the end of all investigated (MAD)derivatives. Consequently, compound (9) lie before (10) and the compound (11) comes at the end of the studied (BAD) inhibitors.

Kinetic-thermodynamic model of the corrosion inhibition

To evaluate the kinetic parameters and correlate them to their corrosion inhibition mechanism, it is now of value to analyze the kinetic data obtained in the presence of the studied mono- and bis-azo dye inhibitors from the stand point of the generalized mechanistic scheme proposed by El-Awady *et al.* [92,93]. The curve fitting of the data for the investigated [(MAD) (1-6)] and [(BAD) (7-11)] inhibitors on iron in 2.0 M HNO₃ and 2.0 M NaOH solutions to the kinetic-thermodynamic model (equation 28) at 303 K.

$$\theta / (1 - \theta) = K' [I]^y \quad (28)$$

$$\text{or} \\ \log (\theta/1-\theta) = \log K' + y \log [I] \quad (29)$$

Where y is the number of inhibitors molecules [I] occupying one active site, and K' is a constant, if relationship (29) is plotted and applicable in Figure 8. As seen, satisfactory linear relation is observed for the studied synthesized azo dye compounds. Hence, the suggested model fits the obtained experimental data. The slope of such lines is the number of inhibitor molecules occupying a single active site, (y) and the intercept is the binding constant ($\log K'$). As mentioned, $1/y$ gives the number of active sites occupied by a single organic molecule and K'^y is the equilibrium constant for the adsorption process. The binding constant (K_b) corresponding to that obtained from the known adsorption isotherms curve fitting is given by the following equation:

$$K_b = K'^{(1/y)} \quad (30)$$

Table 4 comprises the values of $1/y$ and K_b for the studied synthesized azo dye inhibitors. This Table show that the number of active sites occupied by one molecule in the case of either (MAD) and/or (BAD) compounds ($1/y \cong 3 - 53$).

Values of $1/y$ greater than unity implies the formation of multilayer of the inhibitor molecules on the metal surface, whereas, values of $1/y$ less than unity indicates that a given inhibitor molecule will occupy more than one active site [58].

According to the proposed kinetic-thermodynamic model, the adsorption takes place via formation of multilayer of the inhibitor molecules on the iron electrode surface. The slope values do not equal unity (gradient slopes < 1), hence the adsorption of these synthesized azo dye compounds on iron surface does not obey a Langmuir adsorption isotherm [94, 95]. Frumkin adsorption isotherm (equation 15) represents best fit for experimental data obtained from applying these synthesized azo dye compounds as chemical inhibitors on iron in 2.0 M HNO₃ and 2.0 M NaOH solutions. The values of K_{ads} (equilibrium constant of the inhibitor adsorption process) and (f) are tabulated in Table 4. The lateral interaction parameter (f) has negative values, this parameter is a measure of the degree of steepness of the adsorption isotherm. The adsorption equilibrium constant (K_{ads}) calculated from Frumkin equation acquires lower values than those binding constant (K_b) obtained and calculated from the kinetic-thermodynamic model. The lack of compatibility of the calculated (K_b) and experimental (K_{ads}) values may be attributed to the fact that Frumkin adsorption isotherm is only applicable to cases where one active site per inhibitor molecule is occupied. The lateral interaction parameter was introduced to treat of deviations from Langmuir ideal behavior, whereas the kinetic-thermodynamic model uses the size parameter. The values of the lateral interaction parameter ($-f$) were found to be negative and increase from $\cong 23$ to 51. This denotes that, an increase in the adsorption energy takes place with the increase in the surface coverage (θ). Adsorption process is a displacement reaction involving removal of adsorbed water molecules from the electrode metal surface and their substitution by inhibitor molecules. Thus, during adsorption, the adsorption equilibrium forms an important part in the overall free energy changes in the process of adsorption. It has been shown [96] that, the free energy change (ΔG_{ads}°) increases with increase of the solvating energy of adsorbing species, which in turn increases with the size of hydrocarbon portion in the organic molecule and the number of active sites. Hence, the increase of the molecular size leads to decreased solubility, and increased adsorb ability. The large negative values of the standard free energy changes of adsorption (ΔG_{ads}°), obtained for the investigated (MAD) and (BAD) compounds, indicate that the reaction is proceeding spontaneously and accompanied with a high efficient adsorption. Although, the obtained values of the binding constant (K_b) from the kinetic model and the modified equilibrium constant (K_{ads}) from Frumkin equation are incompatible, generally have large values (Table 4), mean better inhibition efficiency of the investigated synthesized (MAD) and (BAD) compounds i.e., stronger electrical interaction between the double layer existing at the phase boundary and the adsorbing molecules. In general, the equilibrium constant of adsorption (K_{ads}) was found to become higher with increasing the inhibition efficiency of the inhibitor studied as shown in Table 4.

CONCLUSIONS

(1) The corrosion behaviour of iron was investigated in 2.0 M HNO₃ and 2.0 M NaOH solutions with and without addition of various concentrations of synthesized mono- and bis-azo dyes, using weight loss, thermometric and electrochemical techniques.

(2) The cathodic and anodic Tafel slopes reveal that the synthesized inhibitors are mixed type (cathodic/anodic) inhibitors in nitric, act mainly as cathodic in sodium hydroxide.

(3) All measurements show that mono- and bis-azo dye inhibitors has excellent inhibition properties for the corrosion of iron in 2.0 M HNO₃ and 2.0 M NaOH at 30°C, and the inhibition efficiency is increased with increasing the concentration of the inhibitor. The three studied methods gave consistent results.

(4) The mechanism of the inhibition processes of the corrosion inhibitors under consideration is mainly the adsorption one, i.e., they are adsorptive inhibitors and their adsorption process obeys the Frumkin adsorption isotherm (θ vs. C_{inh}). This behavior is an agreement with the three applied methods.

(5) The inhibition efficiency depends on the number of adsorption oxygen sites (OH and OMe groups), their charge density and π -electron clouds.

(6) The higher inhibition efficiency of the azo dye additives in acidic than in alkaline media may be due to the less negative potential of Fe in HNO₃, favouring adsorption of the additive.

(7) The large values of the change in the standard free energy of adsorption (ΔG_{ads}°), equilibrium constant (K_{ads}) and binding constant (K_b) revealed that the reactions proceed spontaneously and result in highly efficient physisorption mechanism and stronger electrical interaction between the double layer existing at the phase boundary and the adsorbing molecules. In general, the equilibrium constant of adsorption was found to become higher with increasing inhibition efficiency of the inhibitor tested.

(8) The inhibition efficiency evaluated via theoretical methods was well accorded with reported experimental ones, following the same order as: α -naphthyl- ligand > β -naphthyl > p -anisidine > p -toluidine > o -toluidine > m -toluidine derivative.

References

- [1] Sherif E-SM, Erasmus RM, Comines JD (2010). Effects of 5-(3-Aminophenyl)-tetrazole as a Corrosion Inhibitor on the Corrosion of Mg/Mn alloy in Arabian Gulf Water. *Electrochimica Acta*. 55 (11): 3657-3663.
- [2] Obot I B, Obi-Egbedi NO (2010). Adsorption properties and inhibition of mild steel corrosion in sulphuric acid solution by ketoconazole: Experimental and theoretical investigation". *Corrosion Sci*. 52 (1): 198-204.
- [3] Raja PB, Sethuraman M G (2008). Natural products as corrosion inhibitor for metals, in corrosive media. A review, *Materials Letters*. 62:113– 116.
- [4] Kissi M, Bouklah M, Hammouti B, Benkaddour M (2006). "Establishment of equivalent circuits from electrochemical impedance spectroscopy study of corrosion inhibition of steel by pyrazine in sulphuric acidic solution". *Appl. Surf. Sci*. 252: 4190–4198.
- [5] Tang L, Li X, Mu G, Liu G, Li L, Liu H, Si Y (2006). "The synergistic inhibition between hexadecyltrimethyl ammonium bromide (HTAB) and NaBr for the corrosion of cold rolled steel in 0.5 M sulfuric acid". *J. Mater. Sci*. 41(10): 3063–3069.
- [6] Cruz J, Martínez R, Genesca J, García-Ochoa E (2004). "Experimental and theoretical study of 1-(2-ethylamino)-2-methylimidazole as an inhibitor of carbon steel corrosion in acid media". *J. Electroanalytical Chem*. 566 (1): 111-121.
- [7] Migahed MA (2005). "Electrochemical investigation of the corrosion behaviour of mild steel in 2 M HCl solution in presence of 1-dodecyl-4-methoxypyridinium bromide" *Mater. Chem. Phys*. 93 (1): 48–53.
- [8] Quraishi MA, Ansari FA (2006). "Fatty acid oxadiazoles as corrosion inhibitors for mild steel in formic acid". *J. Appl. Electrochem*. 36 (3): 309– 314.
- [9] Quraishi MA, Rafiquee MZA, Saxena N, Khan S (2006). "Fatty acid oxadiazoles as corrosion inhibitors for mild steel in formic acid ". *J. Corros. Sci. Eng.*: 10–16. doi: 10.1007/s10800-005-9065-z
- [10] Lebrini M, Lagrenée M, Vezin H, Gengembre L, Bentiss F (2005). "Electrochemical and quantum chemical studies of new thiadiazole derivatives adsorption on mild steel in normal hydrochloric acid medium". *Corros. Sci*. 47 (2): 485–505.
- [11] Gece G (2008). "The use of quantum chemical methods in corrosion inhibitor studies". *Corros. Sci*. 50 (11): 2981-2992.
- [12] Obot IB, Obi-Egbedi N O, Odozi NW (2010). "Acenaphtho [1,2-b] quinoxaline as a novel corrosion inhibitor for mild steel in 0.5 M H₂SO₄". *Corros. Sci*. 52 (3): 923-226.
- [13] Obot IB, Obi-Egbedi NO (2010). "2,3-Diphenylbenzoquinoxaline: A new corrosion inhibitor for mild steel in sulphuric acid". *Corros. Sci*. 52 (1): 282–285.
- [14] Obot IB, Obi-Egbedi NO (2008). "Inhibitory Effect and Adsorption Characteristics of 2,3-Diaminonaphthalene At Aluminum/Hydrochloric Acid Interface: Experimental and Theoretical Study". *Surf. Rev. Lett*. 15 (6): 903–910.
- [15] Madkour LH, Zinhome UA (2010). "Inhibition effect of Schiff base compounds on the corrosion of iron in nitric acid and sodium hydroxide solutions". *J. Corrosion Sci. Eng. (JCSE)* 13.
- [16] Bentiss F, Lebrini M, Lagrenée M (2005). "Thermodynamic characterization of metal dissolution and inhibitor adsorption processes in mild steel/2,5-bis(n-thienyl)-1,3,4- thiadiazoles/hydrochloric acid system". *Corros. Sci*. 47 (12): 2915-2931.
- [17] Bentiss F, Gassama F, Barbry D, Gengembre L, Vezin H, Lagrenée M, Traisnel M (2006). "Enhanced corrosion resistance of mild steel in molar hydrochloric acid solution by 1,4-bis(2-pyridyl)-5Hpyridazino[4,5-b]indole: Electrochemical, theoretical and XPS Studies". *Appl. Surf. Sci*. 252 (8): 2684-2691.
- [18] Khaled KF, Babic-Samradzija K, Hackerman N (2005). "Theoretical study of the structural effects of polymethylene amines on corrosion inhibition of iron in acid solutions". *Electrochim. Acta* 50 (12): 2515-2520.
- [19] Lebrini M, Traisnel M, Lagrenée M, Mernari B, Bentiss F (2008). "Inhibitive properties, adsorption and a theoretical study of 3,5-bis(npyridyl)-4-amino-1,2,4-triazoles as corrosion inhibitors for mild steel in perchloric acid". *Corros. Sci*. 50 (2):473-479.
- [20] Madkour LH, Hassanein AM, Ghoneim MM, Eid SA (2001). "Inhibition Effect of Hydantoin Compounds on the Corrosion of Iron in Nitric and Sulfuric Acid Solutions". *Monatshefte für Chemie*. 132 (2): 245-258.
- [21] El-Gaber AS, Madkour LH, El-Askilany AH, Fouda A S (1997). "Inhibition of the acid corrosion of iron with haloacetic acids". *Bulletin of Electrochemistry*. 13 (2): 62-66.
- [22] Madkour LH, Ghoneim MM (1997). "Inhibition of the corrosion of 16/14 austenitic stainless steel by oxygen and nitrogen containing compounds". *Bulletin of Electrochemistry*. 13 (1): 1-7.
- [23] Obot IB, Obi-Egbedi NO (2008). *Colloids and Surfaces A Physicochemical and Engineering Aspects*. 330 (2-3): 207-212.
- [24] Obot IB, Obi-Egbedi NO, Umoren SA (2009). "Adsorption Characteristics and Corrosion Inhibitive Properties of Clotrimazole for Aluminium Corrosion in Hydrochloric Acid". *Int. J. Electrochem. Sci*. 4 (6): 863–877.
- [25] Obot IB, Obi-Egbedi NO (2010). "Adsorption properties and inhibition of mild steel corrosion in sulphuric acid solution by ketoconazole: Experimental and theoretical investigation". *Corros. Sci*. 52 (1): 198–204
- [26] Obot IB, Obi-Egbedi NO, Umoren SA (2009). "Antifungal drugs as corrosion inhibitors for aluminium in 0.1 M HCl". *Corros. Sci*. 51(8):1868– 1875.
- [27] Obot IB, Port (2009). "Synergistic effect of nizoral and iodide ions on the corrosion inhibition of mild steel in sulphuric acid solution". *Electrochim. Acta* 27(5): 539–553.
- [28] Obot IB, Obi-Egbedi NO, Umoren SA (2009). "The synergistic inhibitive effect and some quantum chemical parameters of 2,3-diaminonaphthalene and iodide ions on the hydrochloric acid corrosion of aluminium". *Corros. Sci*. 51(2): 276–282.
- [29] Obot IB, Obi-Egbedi NO (2010). "Theoretical study of benzimidazole and its derivatives and their potential activity as corrosion inhibitors". *Corros. Sci*. 52(2): 657–660.
- [30] Ebenso EE, Alemu H, Umoren SA, Obot IB (2008). "Inhibition of Mild Steel Corrosion in Sulphuric Acid Using Alizarin Yellow GG Dye and Synergistic Iodide Additive". *Int. J. Electrochem. Sci*. 3: 1325–1339
- [31] Ebenso EE (2003). "Effect of halide ions on the corrosion inhibition of mild steel in H₂SO₄ using methyl red: Part 1 ". *Bull. Electrochem*. 19 (5): 209–216.
- [32] Khalil N (2003). "Quantum chemical approach of corrosion inhibition". *Electrochim. Acta* 48 (18): 2635-2640.
- [33] Madkour LH, Issa R M, El-Ghrabawy I M (1999). "Kinetics of substituted bis- and mono-azo dyes as corrosion inhibitors for aluminium in hydrochloric acid and sodium hydroxide solutions". *J. Chem. Res. - Part S*. (7): 408-409. Part M (1999), 1701 - 1726.
- [34] Madkour LH, Elmorsi M A, Ghoneim M M (1995). "Inhibition of copper corrosion by arylazotriazoles in nitric acid solution". *Monatshefte für Chemie Chemical Monthly*. 126 (10): 1087-1095.
- [35] Behpour M, Ghoreis SM, Mohammad N , Soltani N , Salavati-Niasari MM (2010). "Investigation of some Schiff base compounds containing disulfide bond as HCl corrosion inhibitors for mild steel". *Corros. Sci*. 52(12): 4046-4057.
- [36] Obi-Egbedi NO, Obot IB (2011). "Inhibitive properties, thermodynamic and quantum chemical studies of alloxazine on mild steel corrosion in H₂SO₄". *Corros. Sci*. 53 (1): 263-275.
- [37] Li X, Deng S, Mu G, Fu H, Yang F (2008). "Inhibition effect of nonionic surfactant on the corrosion of cold rolled steel in hydrochloric acid". *Corrosion Science*. 50 (2): 420-430.

- [38] Vracar L, Drazic DM (2002). "Adsorption and corrosion inhibitive properties of some organic molecules on iron electrode in sulfuric acid". *Corros. Sci.* 44(8):1669–1680.
- [39] Mylius F Z (1924). *Der Aufbau der Zweist offlegierungen II- Eine kritische Zusammen fassung Metallkunde.* 16: 81.
- [40] Fouda AS, Madkour LH, Elshafei AA, Elasklany AH (1995). "Inhibitory Effect of Some Carbazides on Corrosion of Aluminum in Hydrochloric Acid and Sodium Hydroxide Solutions". *Mat-Wiss, u. Werkstoff tech.* 26: 342-346.
- [41] El-Naggar M M (2007). "Corrosion inhibition of mild steel in acidic medium by some sulfa drugs compounds". *Corrosion Science.* 49 (5): 2226-2236.
- [42] Umoren S A, Ebenso EE (2007). "The synergistic effect of polyacrylamide and iodide ions on the corrosion inhibition of mild steel in H₂SO₄". *Materials Chemistry and Physics.* 106 (2-3): 387-393.
- [43] Lebrini M, Bentiss F, Vezin H, Lagrenée M (2006). "The inhibition of mild steel corrosion in acidic solutions by 2,5-bis(4-pyridyl)-1,3,4- thiadiazole: Structure–activity correlation". *Corros. Sci.* 48(5):1279 - 1291.
- [44] Musa AY, Khadom AA, Kadhum AH, Mohamad AB, Takriff MS (2010). "Kinetic behavior of mild steel corrosion inhibition by 4-amino-5- phenyl-4H-1,2,4-trizole-3-thiol". *J. Taiwan, Ins. Chem. Eng.* 41(1): 126–128.
- [45] Khadom AA, Yaro AS, Kadum AH, Taiwan J (2010). "Corrosion inhibition by naphthylamine and phenylenediamine for the corrosion of copper-nickel alloy in hydrochloric acid". *Ins. Chem. Eng.* 41(1):122–125.
- [46] Bouklah M, Hammouti B, Lagrenée M, Bentiss F (2006). "Thermodynamic properties of 2,5-bis(4-methoxyphenyl)-1,3,4-oxadiazole as a corrosion inhibitor for mild steel in normal sulfuric acid medium". *Corros. Sci.* 48(9): 2831–2842.
- [47] Chitra S, Parameswari K, Sivakami C, Selvaraj A (2010). "Sulpha Schiff Bases as Corrosion Inhibitors for Mild Steel in 1M Sulphuric Acid". *Chem. Eng. Res. Bull.* 14: 1–6.
- [48] Zou Y, Wang J, Zheng YY (2011). "Electrochemical techniques for determining corrosion rate of rusted steel in seawater". *Corrosion Science.* 53 (1): 208-216.
- [49] Solomon M M, Umoren S A, Udosoro II, Udoh AP (2010). "Inhibitive and adsorption behaviour of carboxymethyl cellulose on mild steel corrosion in sulphuric acid solution". *Corrosion Science.* 52 (4): 1317-1325.
- [50] Fainerman VB, Lylyk SV, Aksenenko EV, Makievski AV, Petkov JT, Yorke J, Miller R (2009). *Colloids and Surfaces A Physicochemical and Engineering Aspects.* 334 (3): 1-7.
- [51] Bentiss F, Jama C, Mernari B, Attari HE, Kadi LE, Lebrini M, Traisnel M, Lagrenée M (2009). "Corrosion control of mild steel using 3,5-bis(4-methoxyphenyl)-4-amino-1,2,4-triazole in normal hydrochloric acid medium". *Corrosion Science.* 51 (8) : 1628-1635.
- [52] Benali O, Larabi L, Traisnel M, Gengembra L, Harek Y (2007). "Corrosion inhibition efficiency and surface activity of benzothiazol-3-ium cationic Schiff base derivatives in hydrochloric acid". *Applied Surface Science.* 253 (14): 6130-6139.
- [53] Bentiss F, Lebrini M, Lagrenée M (2005). "Thermodynamic characterization of metal dissolution and inhibitor adsorption processes in mild steel/2,5-bis(n-thienyl)-1,3,4-thiadiazoles/hydrochloric acid system". *Corrosion Sci.* 52 (6): 2122-2132.
- [54] Negm NA, Elkholy YM, Zahran MK, Tawfik SM (2010). "Corrosion inhibition efficiency and surface activity of benzothiazol-3-ium cationic Schiff base derivatives in hydrochloric acid". *Corrosion Sci.* 52 (6): 2123-2136.
- [55] Abiola OK, Otaigbe JOE (2009). "The effects of Phyllanthus amarus extract on corrosion and kinetics of corrosion process of aluminum in alkaline solution". *Corros. Sci.* doi:10.1016/j.corsci. 2009.07.006
- [56] Emregul KC, Hayvali M (2006). "Studies on the effect of a newly synthesized Schiff base compound from phenazone and vanillin on the corrosion of steel in 2 M HCl". *Corros. Sci.* 48 (4): 797–812.
- [57] Bouklah M, Hammouti B, Lagrenée M, Bentiss F (2006). "Thermodynamic properties of 2,5-bis(4-methoxyphenyl)-1,3,4-oxadiazole as a corrosion inhibitor for mild steel in normal sulfuric acid medium". *Corrosion Sci.* 48 (9): 2831-2842.
- [58] Frumkin AN (1925). "Surface tension curves of higher fatty acids and the equation of condition of the surface layer". *Z. Phys. Chem.*, 116: 466-484.
- [59] Babić-Samardžija K, Khaled KF, Hackerman N (2005). "Investigation of the inhibiting action of O-, S- and N-dithiocarbamate(1,4,8,11 tetraazacyclotetradecane) cobalt(III) complexes on the corrosion of iron in HClO₄ acid". *Applied Surface Sci.* 240 (1-4): 327-340.
- [60] Sankarapavinasam S, Ahmed MF (1992). "BENZENETHIOLS AS INHIBITORS FOR THE CORROSION OF COPPER". *J. Appl Electrochemistry.* 22 (4): 390-395.
- [61] El-Sayed AR (1998). "The Inhibition Effect of Some Nitrogen-heterocyclic Compounds on Corrosion of Aluminium and Its Alloys in HCl Solution". *Denki Kagaku.* 66 (2): 176-185.
- [62] Khaled KF, Hackerman N (2004). "Ortho-substituted anilines to inhibit copper corrosion in aerated 0.5 M hydrochloric acid". *Electrochimica Acta.* 49 (3): 485-495.
- [63] Abd El-Maksoud S A, Fouda AS (2005). "Some pyridine derivatives as corrosion inhibitors for carbon steel in acidic medium". *Materials Chemistry and Physics.* 93 (1): 84-90.
- [64] Ahamad I, Prasad R, Quraishi MA (2010). "Thermodynamic, electrochemical and quantum chemical investigation of some Schiff bases as corrosion inhibitors for mild steel in hydrochloric acid solutions". *Corrosion Sci.* 52 (3): 933-942.
- [65] Avci G (2008). "Corrosion inhibition of indole-3-acetic acid on mild steel in 0.5 M HCl". *Colloids Surf. A* 317 (1-3): 730–736
- [66] Quartarone G, Bonaldo L, Tortato C (2006). "Inhibitive action of indole-5-carboxylic acid towards corrosion of mild steel in deaerated 0.5 M sulfuric acid solutions". *Appl. Surf. Sci.* 252 (23): 8251–8257.
- [67] Chauhan LR, Gunasekaran G (2007). "Corrosion inhibition of mild steel by plant extract in dilute HCl medium". *Corrosion Sci.* 49 (3): 1143- 1161.
- [68] Hegazy MA (2009). "A novel Schiff base-based cationic gemini surfactants: Synthesis and effect on corrosion inhibition of carbon steel in hydrochloric acid solution". *Corrosion Sci.* 51 (11): 2610-2618.
- [69] Adriana Barbosa da Silva, Eliane D'Elia, José Antonio da Cunha Ponciano Gomes (2010). "Carbon steel corrosion inhibition in hydrochloric acid solution using a reduced Schiff base of ethylenediamine". *Corrosion Sci.* 52 (3): 788-793.
- [70] Bayol E, Kayakirilmaz K, Erbil M (2007). "The inhibitive effect of hexamethylenetetramine on the acid corrosion of steel". *Materials Chemistry and Physics.* 104 (1): 74-82.
- [71] Noor EA, Al-Moubaraki AH (2008). "Thermodynamic study of metal corrosion and inhibitor adsorption processes in mild steel/1-methyl-4[4'(- X)-styryl]pyridinium iodides/hydrochloric acid systems". *Materials Chemistry and Physics.* 110 (1): 145-154.
- [72] Bentiss F, Jama C, Mernari B, Attari HE, Kadi LE, Lebrini M, Traisnel M, Lagrenée M (2009). "Corrosion control of mild steel using 3,5-bis(4-methoxyphenyl)-4-amino-1,2,4-triazole in normal hydrochloric acid medium". *Corrosion Sci.* 51 (8): 1628-1635.
- [73] Valcarce MB, Vázquez M (2009). "Carbon steel passivity examined in solutions with a low degree of carbonation: The effect of chloride and nitrite ions". *Materials Chemistry and Physics.* 115 (1): 313-321.

- [74] Noor EA, Al-Moubaraki AH (2008). "Thermodynamic study of metal corrosion and inhibitor adsorption processes in mild steel/1-methyl-4[4'(- X)-styryl]pyridinium iodides/hydrochloric acid systems". *Materials Chemistry and Physics*, 110 (1): 145-154.
- [75] Şahin M, Bilgiç S, Yılmaz H (2002). "The inhibition effects of some cyclic nitrogen compounds on the corrosion of the steel in NaCl mediums". *Applied Surface Sci.* 195 (1-4): 1-7.
- [76] Umoren SA, Ogbobe O, Igwe IO, Ebenso EE (2008). "Inhibition of mild steel corrosion in acidic medium using synthetic and naturally occurring polymers and synergistic halide additives". *Corrosion Sci.* 50 (7): 1998-2006.
- [77] Khaled KF (2004). "An electrochemical study for corrosion inhibition of iron by some organic phosphonium chloride derivatives in acid media". *Applied Surface Sci.* 230 (1-4): 307-318.
- [78] Solomon MM, Umoren SA, Udoso II, Udoh AP (2010). "Inhibitive and adsorption behaviour of carboxymethyl cellulose on mild steel corrosion in sulphuric acid solution". *Corrosion Sci.* 52 (4): 1317-1325.
- [79] Badawy WA, Ismail K M, Fathi AM (2006). "Corrosion control of Cu-Ni alloys in neutral chloride solutions by amino acids". *Electrochimica Acta.* 51 (20): 4182-4189.
- [80] Abdallah M (2002). "Rhodanineazosulpha drugs as corrosion inhibitors for corrosion of 304 stainless steel in hydrochloric acid solution". *Corrosion Sci.* 44 (4): 717-728.
- [81] Tang L, Li X, Si Y, Mu G, Liu G (2006). "The synergistic inhibition between 8-hydroxyquinoline and chloride ion for the corrosion of cold rolled steel in 0.5 M sulfuric acid". *Materials Chemistry and Physics.* 95 (1): 29-38.
- [82] Sibel Z, Dogan P, Yazici B (2005). "Acidic corrosion of iron and aluminum by SDBS at different temperatures". *Corros.Rev.* 23: 217.
- [83] Singh AK, Quraishi M A (2010). "The effect of some bis-thiadiazole derivatives on the corrosion of mild steel in hydrochloric acid". *Corrosion Sci.* 52 (4): 1373-1385.
- [84] Soltani N, Behpour M, Ghoreishi SM, Naeimi H (2010). "Corrosion inhibition of mild steel in hydrochloric acid solution by some double Schiff bases". *Corrosion Sci.* 52 (4): 1351-1361.
- [85] Ramesh SV, Adhikari AV (2008). "Quinolin-5-ylmethylene-3-[[8-(trifluoromethyl)quinolin-4-yl]thio]propanohydrazide as an effective inhibitor of mild steel corrosion in HCl solution". *Corros. Sci.* 50 (1): 55-61.
- [86] Musa AY, Kadhum AAH, Mohamad AB, Daud AR, Takriff MS, Kamarudin SK (2009). "A comparative study of the corrosion inhibition of mild steel in sulphuric acid by 4,4-dimethylloxazolidine-2-thione". *Corrosion Sci.* 51 (10): 2393-2399.
- [87] Behpour M, Ghoreishi SM, Soltani N, Salavati-Niasari M, Hamadani M, Gandomi A (2008). "Electrochemical and theoretical investigation on the corrosion inhibition of mild steel by thiosalicylaldehyde derivatives in hydrochloric acid solution". *Corrosion Sci.* 50 (8): 2172-2181.
- [88] Benali O, Larabi L, Traisnel M, Gengembre L, Harek Y (2007). "Electrochemical, theoretical and XPS studies of 2-mercapto-1- methylimidazole adsorption on carbon steel in 1 M HClO₄". *Applied Surface Sci.* 253 (14): 6130-6139.
- [89] Noor EA, Al-Moubaraki AH (2008). "Thermodynamic study of metal corrosion and inhibitor adsorption processes in mild steel/1-methyl-4[4'(- X)-styryl]pyridinium iodides/hydrochloric acid systems". *Materials Chemistry and Physics.* 110 (1): 145-154.
- [90] Emregül KC, Hayvalı M (2006). "Studies on the effect of a newly synthesized Schiff base compound from phenazone and vanillin on the corrosion of steel in 2 M HCl". *Corrosion Sci.* 48 (4): 797-812.
- [91] Leçe HD, Emregül K C, Atakol O (2008). "Difference in the inhibitive effect of some Schiff base compounds containing oxygen, nitrogen and sulfur donors". *Corrosion Sci.* 50 (5): 1460-1468.
- [92] El-Awady AN A, Abd-El-Nabey BA, Aziz SG, Khalifa M, Al-Ghamedy HA (1990). "Kinetics and Thermodynamics of the Inhibition of the Acid Corrosion of Steel by Some Macrocyclic ligands". *Int. J. Chem.* 1(4): 169-179.
- [93] El-Awady AA, Abd-El-Nabey BA, Aziz SG (1992). —Kinetic-Thermodynamic and Adsorption Isotherms Analyses for the Inhibition of the Acid Corrosion of Steel by Cyclic and Open-Chain Amines. *J. Electrochem. Soc.* 139 (8): 2149-2154.
- [94] Fouda AS, Moussa MN, Taha FI, Elneanaa AI (1986). "The role of some thiosemicarbazide derivatives in the corrosion inhibition of aluminium in hydrochloric acid". *Corrosion Sci.* 26 (9): 719-726.
- [95] Langmuir I (1918). "The adsorption of gases on plane surface of glass, mica and platinum". *J. Amer. Chem. Soc.* 40:1361-1403.
- [96] Szkarska-Smialowska Z, Dus B (1967). "Effect of Some Organic Phosphorus Compounds on the Corrosion of Low Carbon Steel in Hydrochloric Acid Solutions" *Corrosion* 23: 130.